CAPTURING PLANAR TIRE PROPERTIES USING STATIC CONSTRAINT MODES

Rui Ma
Mechanical Engineering Department
Virginia Tech
Danville, VA 24540
rainfall@vt.edu

Alexander A. Reid, Ph.D.
U.S. Army RDECOM-TARDEC
Senior Engineer, Motion Base Technologies Team
RDTA-RS-CA-HMS #157
Warren, MI 48397
alexander.a.reid@us.army.mil

John B. Ferris
Mechanical Engineering Department
Virginia Tech
Danville, VA, 24540
jbferris@vt.edu

ABSTRACT

The interaction between the tire and road has long been of interest for vehicle dynamic simulation. A planar tire model is developed to capture the tire circumferential displacements and calculate the spindle force according to the tire shape. The tire is discretized into segments and Hamilton's principle is used to derive the model mathematical expression. It is shown that the static constraint modes are functions of two non-dimensional parameters; a third parameter defines the overall stiffness. These parameters are experimentally identified for a specific tire. The bridging and enveloping properties are examined circumferentially. The prediction accuracy of spindle force with respect to tire-road interference is evaluated by comparing the simulation and experimental response for a quasi-static cleat test. The simulation result of spindle force agrees with the experimental data and the process can be implemented as a morphological pre-filter of road profiles for more efficient vehicle modeling and simulation.

NOMENCLATURE

k Distributed spring rate.
u Radial deflection.
R Tire radius.
$\mathbf{\Psi^{ac}}$ Vector of active constraint degrees of freedom.
$\mathbf{\Phi^{c}}$ Matrix of constraint modes.
$F_{\Delta\theta}$ Force acting on one single tire piece.
f Linear distributed load density.
l length of one single tire piece.
$\Delta\theta$ Angular range of each tire segment.
V_b Bending potential energy for each tire segment.
σ_{xx} Elastic stress for each tire segment.
ε_{xx} Elastic strain for each tire segment.

Report Documentation Page

Form Approved
OMB No. 0704-0188

1. REPORT DATE **13 MAR 2012**	2. REPORT TYPE **Journal Article**	3. DATES COVERED **22-11-2011 to 20-02-2012**

4. TITLE AND SUBTITLE **CAPTURING PLANAR TIRE PROPERTIES USING STATIC CONSTRAINT MODES**	5a. CONTRACT NUMBER 5b. GRANT NUMBER 5c. PROGRAM ELEMENT NUMBER
6. AUTHOR(S) **Rui Ma; Alexander Reid; John Ferris**	5d. PROJECT NUMBER 5e. TASK NUMBER 5f. WORK UNIT NUMBER
7. PERFORMING ORGANIZATION NAME(S) AND ADDRESS(ES) **Mechanical Engineering Department,Virginia Tech,965 Prices Fork Road,Danville,VA,24540**	8. PERFORMING ORGANIZATION REPORT NUMBER **; #22647**
9. SPONSORING/MONITORING AGENCY NAME(S) AND ADDRESS(ES) **U.S. Army RDECOM-TARDEC, 6501 East Eleven Mile Rd, RDTA-RS-CA-HMS #157, Warren, Mi, 48397-5000**	10. SPONSOR/MONITOR'S ACRONYM(S) **TARDEC** 11. SPONSOR/MONITOR'S REPORT NUMBER(S) **#22647**

12. DISTRIBUTION/AVAILABILITY STATEMENT
Approved for public release; distribution unlimited

13. SUPPLEMENTARY NOTES

14. ABSTRACT
The interaction between the tire and road has long been of interest for vehicle dynamic simulation. A planar tire model is developed to capture the tire circumferential displacements and calculate the spindle force according to the tire shape. The tire is discretized into segments and Hamilton?s principle is used to derive the model mathematical expression. It is shown that the static constraint modes are functions of two non-dimensional parameters; a third parameter defines the overall stiffness. These parameters are experimentally identified for a specific tire. The bridging and enveloping properties are examined circumferentially. The prediction accuracy of spindle force with respect to tire-road interference is evaluated by comparing the simulation and experimental response for a quasi-static cleat test. The simulation result of spindle force agrees with the experimental data and the process can be implemented as a morphological pre-filter of road profiles for more efficient vehicle modeling and simulation.

15. SUBJECT TERMS

16. SECURITY CLASSIFICATION OF:			17. LIMITATION OF ABSTRACT	18. NUMBER OF PAGES	19a. NAME OF RESPONSIBLE PERSON
a. REPORT **unclassified**	b. ABSTRACT **unclassified**	c. THIS PAGE **unclassified**	**Public Release**	**7**	

Standard Form 298 (Rev. 8-98)
Prescribed by ANSI Std Z39-18

M Bending moment for each tire segment.

E Elastic modulus.

I Second moment of area for each tire segment.

ρ Massive density.

γ Shear strain.

V_s Shear potential energy for each tire segment.

G Shear modulus.

T Kinetic energy for each tire segment.

V_e Elastic potential energy for each tire segment.

W External work on each tire segment.

n Tire segment number.

INTRODUCTION

The interaction between the tire and road has long been of interest for vehicle dynamic simulation and chassis design. Therefore, a proper tire model that captures the circumferential deformation and predicts the load is required. The tire model should bridge cracks in the pavement and envelope small bumps, and the resultant force should be obtainable through the circumferential deformation. A considerable amount of research has been done in this area. Umsrithong presents a detailed tire model review in his dissertation[1]. Among all kinds of tire models, the in-plane ring model with elastic foundation places most emphasis on the circumferential deformation. Badalamenti et al. developed the radial spring tire model, which makes the radial spring element deflection dependent on the adjacent element deflections[2]. This model is shown to accurately describe the tire envelopment behavior. Zegelaar and Pacejka used a flexible ring model to simulate the quasi-static response of a tire rolling over an uneven surface[3]. The simulation results agreed with experimental data, but the complexity of the model increases the computational requirements. Loo modeled the tire by using a flexible circular ring under tension with a nest of linear springs and dampers arranged radially[4]. The ring tension and foundation stiffness are obtained by experimental data from a static point-load test and the contact patch measurements. This model takes tire rolling resistance into consideration. Gillespie used a simple radial spring model to simulate the stiffness variation circumferentially[5]. The magnitude of the radial force variation is found to be relatively independent of speed. Takayama et al. developed a mass-spring tire model to predict the transient response of a tire encountering a cleat [6]. The belt and tread region was modeled by a rigid ring and deflections from the cleat are absorbed by a linear and planar spring attached to the rigid ring.

Ferris proposed the static constraint mode tire model to capture the tire enveloping properties[7]. The model applies an iterative process to identify the active constraints at the tire-road interface from which the resulting circumferential deformation of the tire is formulated. This work developed in this paper improves on this static constraint mode model. The theory is expanded to include shear effects and the required stiffness parameters are reduced from five dependent parameters to two parameters that define the constraint modes and an independent parameter that defines the overall tire stiffness. In this way the parameters that define the shape of the tire are independent from the overall stiffness. The ability of the model to generate the correct tire shape is validated for cracks and bumps to check the enveloping and bridging properties. The appropriate overall tire stiffness parameter is identified through the experimental result from a single flat-plate test. The resultant spindle force can be calculated through the circumferential displacement. A set of experimental quasi-static cleat tests are used to validate the entire modeling process.

The work is organized as follows: First the background on the constraint mode method is reviewed. Next the improved theoretical deduction process of the constraint mode model is developed. The model parameters are then identified via the deformed tire shape and validated with experimental data. The bridging and enveloping properties of the model are examined to check the effectiveness of the model in terms of circumferential deformation. Finally, the simulation result of spindle force versus deformation over a cleat is compared with experimental data to demonstrate the force prediction accuracy.

BACKGROUND

Since the development of component mode synthesis originated by Hurty and Gladwell, the reduced representation of component model has long been of interest in developing component constraint modes [8, 9]. Guyan provides a static reduction method for mass and stiffness matrices [10], from which Kuhar and Stahle developed the dynamic transformation method to derive constraint modes from the response at a given frequency [11]. Ferris proposed a constraint mode tire model to describe the static deflection where the system is assumed to be adequately represented by an undamped, second order, linear, time invariant, ordinary differential equation as given in Eq. (1).

$$[\mathrm{m}]\{\ddot{\mathrm{u}}\} + [\mathrm{k}]\{\mathrm{u}\} = \{\mathrm{f}\} \tag{1}$$

The physical degrees of freedom can be categorized into active and omitted ones, represented by ‘a’ and ‘o’ respectively.

In general, the boundary degrees of freedom must be a subset of the active degrees of freedom. In the tire modeling case, the active degrees of freedom must include those in contact with the terrain. Therefore the mass and stiffness matrices are reordered and partitioned as given in Eq. (2).

$$\{\boldsymbol{u}\} = \begin{Bmatrix} \{\boldsymbol{u}^a\} \\ \{\boldsymbol{u}^o\} \end{Bmatrix}$$
$$[\boldsymbol{m}] = \begin{bmatrix} [\boldsymbol{m}^{aa}] & [\boldsymbol{m}^{ao}] \\ [\boldsymbol{m}^{oa}] & [\boldsymbol{m}^{oo}] \end{bmatrix}$$
$$[\boldsymbol{k}] = \begin{bmatrix} [\boldsymbol{k}^{aa}] & [\boldsymbol{k}^{ao}] \\ [\boldsymbol{k}^{oa}] & [\boldsymbol{k}^{oo}] \end{bmatrix} \tag{2}$$

By substituting Equation 2 into Equation 1, and following the work by Kuhar and Stahle, the constraint frequency ω_c^2 and the constraint modes $\{\Psi\}_i$ can be computed as shown in Eq. (3).

$$\left(\begin{bmatrix} [\boldsymbol{k}^{aa}] & [\boldsymbol{k}^{ao}] \\ [\boldsymbol{k}^{oa}] & [\boldsymbol{k}^{oo}] \end{bmatrix} - \omega_c^2 \begin{bmatrix} [\boldsymbol{m}^{aa}] & [\boldsymbol{m}^{ao}] \\ [\boldsymbol{m}^{oa}] & [\boldsymbol{m}^{oo}] \end{bmatrix}\right) \begin{Bmatrix} \{\boldsymbol{\Psi}^{ac}\} \\ \{\boldsymbol{\Psi}^{oc}\} \end{Bmatrix} = \begin{Bmatrix} \{\boldsymbol{f}\} \\ \{\boldsymbol{0}\} \end{Bmatrix} \tag{3}$$

The lower set of equations can be used to derive the constraint mode matrix given in Eq. (4).

$$\begin{Bmatrix} \{\boldsymbol{\Psi}^{ac}\} \\ \{\boldsymbol{\Psi}^{oc}\} \end{Bmatrix} = \begin{bmatrix} [\boldsymbol{I}] \\ -([\boldsymbol{k}^{oo}] - \omega_c^2[\boldsymbol{m}^{oo}])^{-1}([\boldsymbol{k}^{oa}] - \omega_c^2[\boldsymbol{m}^{oa}]) \end{bmatrix} \{\boldsymbol{\Psi}^{ac}\} = [\boldsymbol{\Phi}^c]\boldsymbol{\Psi}^{ac} \tag{4}$$

The active constraint degrees of freedom $\{\Psi^{ac}\}$ are defined by iteratively applying the unilateral geometric constraints at the tire-road interface [7].

The tire is assumed to be axisymmetric and isotropic circumferentially. A simple model which captures the essential in-plane tire behavior is shown as Figure 1. The tire is modeled as an inextensible ring supported by an elastic foundation representing the radial stiffness. The tire is divided into n segments and analyzed discretely as Figure 2 shows. Each individual tire segment is considered as an Euler elastic beam. $\{u\}$ is the radial deflection used to describe the circumferential tire displacement. A recursive algorithm to determine the active geometric constraint is developed in Ferris' work [7].

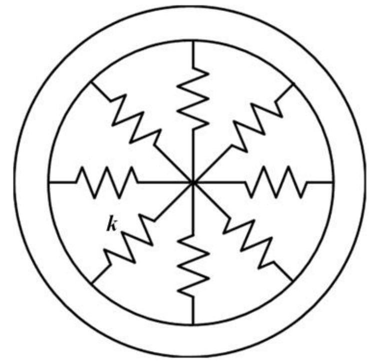

FIGURE 1. IN-PLANE TIRE MODEL SCHEME

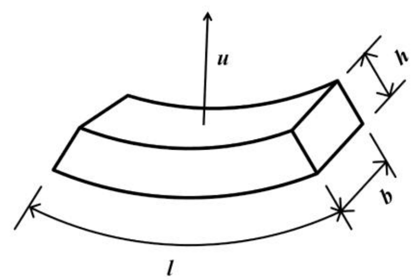

FIGURE 2. TIRE RING SEGMENTS IN 3D

MODEL DEVELOPMENT

In order to examine the relationship between the stiffness matrix and the tire properties, a more detailed expression of the model is required. The shear potential energy term is added to Ferris's constraint mode deduction [7] to describe the relative movement of two adjacent tire segments. Therefore the equation resulting from the application of Hamilton's principle for one tire segment can be rewritten as Eq. (5).

$$\int_{t_1}^{t_2} (\delta T - \delta V_b - \delta V_e - \delta V_s + \delta W)dt = 0 \qquad \forall t_1, t_2 \tag{5}$$

The kinetic energy term vanishes under the quasi-static assumption. Each term and the corresponding virtual changes are computed as Eq. (6) - Eq. (10) :

$$T = \frac{1}{2}\rho l\left(\frac{\partial u}{\partial t}\right)^2 = 0 \qquad \delta T = 0 \tag{6}$$

$$V_b = \frac{EIl}{2}\left(\frac{\partial^2 u}{\partial x^2}\right)^2 \qquad \delta V_b = EIl\frac{\partial^4 u}{\partial x^4}\delta u \tag{7}$$

$$V_e = \frac{1}{2}klu^2 \qquad \delta V_e = klu\delta u \tag{8}$$

$$V_s = \frac{Gblh}{2}\left(\frac{\partial u}{\partial x}\right)^2 \qquad \delta V_s = Glbh\frac{\partial^2 u}{\partial x^2}\delta u \tag{9}$$

$$W = flu \qquad \delta W = fl\delta u \tag{10}$$

The equation of motion for each segment is then simplified to Eq. (11).

$$EIl\frac{\partial^4 u}{\partial x^4} + klu + Glbh\frac{\partial^2 u}{\partial x^2} = \mathrm{fl} \tag{11}$$

The solution to Eq. (11), assuming that the solution is separable in space and time, can be expressed as Eq. (12).

$$u_{(x,t)} = V_x e^{\lambda t} \tag{12}$$

Therefore the fourth derivative with respected to x can be expressed as Eq. (13).

$$\frac{\partial^4 u}{\partial x^4} = V_x'''' e^{\lambda t} \tag{13}$$

The derivatives of V_0 with respect to x at point zero, i.e., the derivative of u with respect to x, can be approximated by adjacent points with finite difference method. Eq. (14) shows the approximation of V_0'''' with 2 adjacent points on each side.

$$u_0'''' \simeq \frac{u_{-2} - 4u_{-1} + 6u_0 - 4u_1 + u_2}{l^4} \tag{14}$$

By substituting Eq.(14), Eq. (11) is transformed into Eq. (15).

$$Au_{n-1} + (B - 4A)u_n + (6A - 2B + C)u_0 + (B - 4A)u_1 + Au_2 = F_{\Delta\theta} \tag{15}$$

Where

$$A = \frac{EI}{l^3} = \frac{EIn^3}{(2\pi R)^3}$$ Bending stiffness parameter

$$B = \frac{Gbh}{l} = \frac{Gbhn}{2\pi R}$$ Shear stiffness parameter

$$C = kl = \frac{2k\pi R}{n}$$ Elastic stiffness parameter

$$F_{\Delta\theta} = \frac{2f\pi R}{n}$$ Force on each tire segment

In this work, the system is assumed to be quasi-static, therefore the constraint frequency is zero and Eq. (4) reduces to the Guyan form where the circumferential displacements of the tire can be predicted by Eq. (16).

$$\begin{Bmatrix} \{\Psi^{ac}\} \\ \{\Psi^{oc}\} \end{Bmatrix} = \begin{bmatrix} [I] \\ -([k^{oo}])^{-1}[k^{oa}] \end{bmatrix} \{\Psi^{ac}\} = [\Phi^c]\{\Psi^{ac}\} \tag{16}$$

The stiffness matrix [k] has the following form.

$$[k] = k_0 \begin{bmatrix} 1 & \alpha_1 & \alpha_2 & 0 & \cdots & \alpha_2 & \alpha_1 \\ \alpha_1 & 1 & \alpha_1 & \alpha_2 & \cdots & 0 & \alpha_2 \\ \alpha_2 & \alpha_1 & 1 & \alpha_1 & \vdots & 0 & 0 \\ 0 & \alpha_2 & \alpha_1 & 1 & \cdots & 0 & 0 \\ \vdots & \vdots & \vdots & \vdots & \vdots & \vdots & \vdots \\ \alpha_1 & \alpha_2 & 0 & 0 & \cdots & \alpha_1 & 1 \end{bmatrix} = k_0[\alpha] \tag{17}$$

Where $k_0 = 6A - 2B + C, \alpha_1 = B - 4A, \alpha_2 = A$

Eq. (17) can be reordered as:

$$k_0 \begin{bmatrix} \alpha^{ao} & a^{aa} \\ \alpha^{oa} & \alpha^{oo} \end{bmatrix} \begin{Bmatrix} u^a \\ u^o \end{Bmatrix} = \begin{Bmatrix} F^{aa} \\ 0 \end{Bmatrix} \tag{18}$$

It can be seen that the resultant tire shape depends on α^{oo} and α^{oa}, therefore the parameters α_1 and α_2 completely determine the constraint modes and together with the active degrees of freedom completely specify the radial tire deformation. The parameter k_0 is an overall stiffness coefficient used to tune a specific tire. The constraint model parameters must be estimated and adjusted according to mechanical properties of different tires. A parameter identification process is necessary so that the model can be applied to force predictions of different tires with a consistent practice of identifying the set of modal parameter values.

PARAMETER IDENTIFICATION PROCESS

The experimental data used throughout this work is provided by Professor Schalk Els of the University of Pretoria, South Africa. The tire used is Continental Conti-Trac AT 238/85 R16 and the schematic experiment set up is shown as

Figure 4. During the Parameter Identification Process, a flat plate is pushed towards the center of the tire gradually and the resultant spindle force F is measured with respect to the tire-plate interference e. No data was available for the deformed shape of the tire, so the parameters α_1 and α_2 are estimated by trial and error practice so that the tire maintains a reasonable deformed shape. The results of this choice of shape parameters are developed in the Validation section of this work.

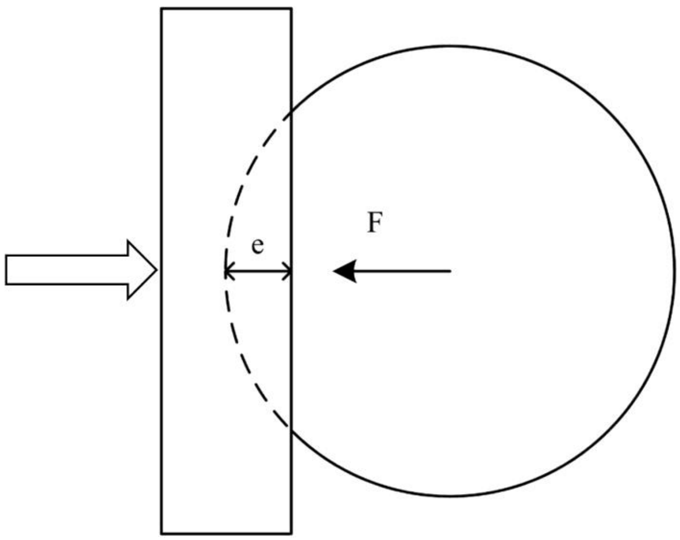

FIGURE 4. SCHEME OF TIRE FLAT-PLATE TEST SETUP

An optimization process with respect to the difference between the simulated and the experimental forces is employed to identify the overall stiffness parameter, k_0, for a specific tire. The comparison between the simulated result and the experimental data shows very good agreement as indicated in Figure 5. The model parameters for the specific tire used in this work given the number of finite segments, n, is provided in Table 1. There were 72 segments used in this work.

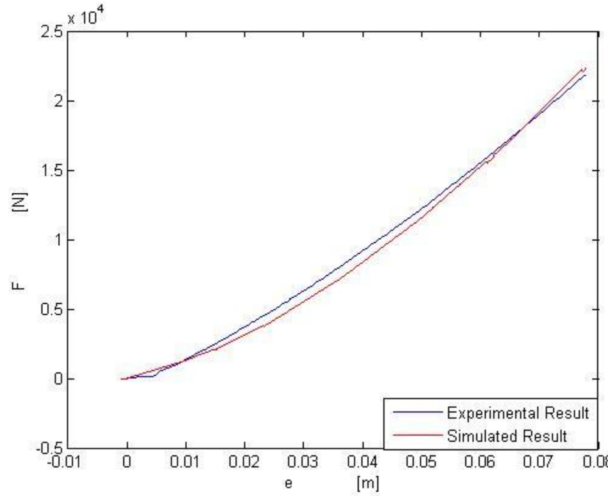

FIGURE 5. COMPARISON BETWEEN THE FLAT-PLATE EXPERIMENTAL AND SIMULATED FORCE, F, WITH RESPECT TO THE INTERFERENCE, E.

TABLE 1. TIRE SHAPE AND STIFFNESS PARAMETERS FOR A PARTICULAR TIRE

Parameters	Values
$\boldsymbol{\alpha_1}$	$1388.8889n - 12.8601n^3$
$\boldsymbol{\alpha_2}$	$3.2150n^3$
$\boldsymbol{k_0}$	$19.2301n^3 - 2777.7778n + 5400000\frac{1}{n}$

VALIDATION

The tire model can be tested over small cracks and bumps using the tire shape parameters, α_1 and α_2, listed in Table 1. The resultant shapes are shown in Figure 6. The black and the red lines represent the original and deformed tire shape respectively, while the blue lines represent the discretized terrain profile. The tire bridging and enveloping properties are evident.

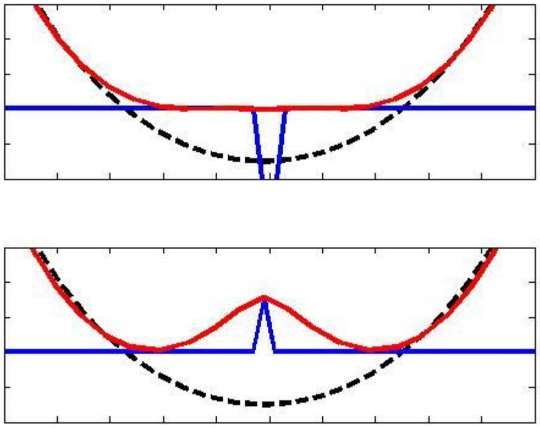

FIGURE 6. BRIDGING AND ENVELOPING PROPERTIES OF CONSTRAINT MODE TIRE MODEL

A cleat test is conducted using the test layout as shown in Figure 7. A flat plate with a square tube at the center is pushed gradually towards of the tire and the resultant spindle force F is measured with respect to the tire-plate interference e. The side length of the square tube is 19 mm.

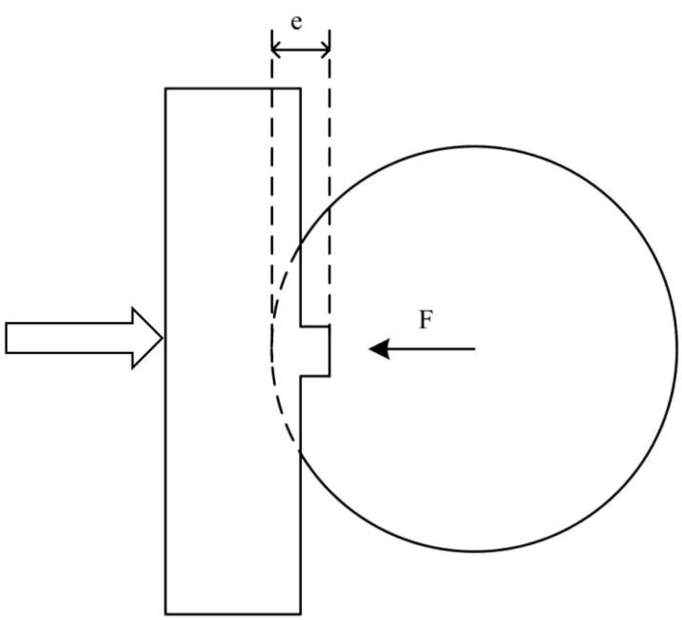

FIGURE 7. SCHEME OF TIRE CLEAT TEST SETUP

The comparison between the simulation and measured data shows reasonable agreement in linear region, i.e. the small interference region (up to 0.05m), as shown in Figure 8. It appears that the stiffness parameter, k_0, that was identified using a flat plate underestimates the stiffness for a cleat test. This may be due to the fact that the shape of the tire during the flat plate test is unknown. A better estimate of the tire shape parameters, α_1 and α_2, may in turn lead to a better estimate of the stiffness parameter. The force versus deflection curve as shown in Figure 8 shows a discontinuity in slope when the deflection is around 0.047 m. In the first segment with smaller slope, the tire is suspended by the cleat event in the air and the contact area related to force generation is constrained to the cleat surface only. The ground does not provide any support at this point. Therefore the force change rate with respect to deflection is relatively small. In the second segment with a larger slope, the tire tread outside the cleat contact area touches the ground and the contact area increases. The ground starts to provide vertical support force to the tire. Therefore the rate at which the generated force changes with respect to the deflection increases.

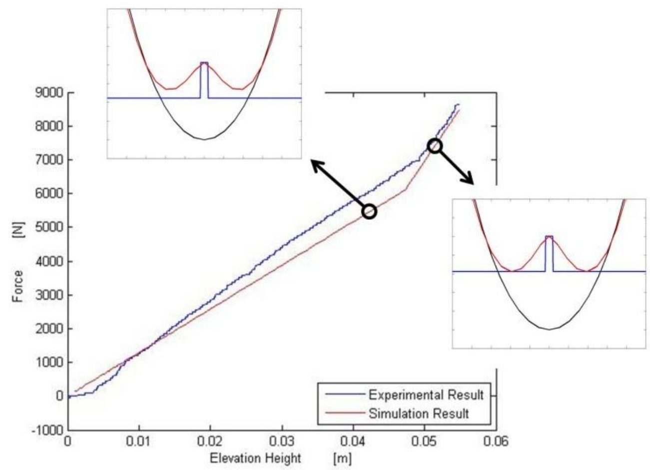

FIGURE 8. COMPARISON BETWEEN THE CLEAT EXPERIMENTAL AND SIMULATED FORCE, F, WITH RESPECT TO THE INTERFERENCE, E.

DISCUSSION

The constraint mode model can serve as a morphological pre-filter of actual terrain since it incorporates the enveloping and bridging property. That is, the wheel trajectory can be computed given a section of actual terrain profile over which the wheel travels and a constant spindle load. Figure 9 shows the comparison between the actual terrain profile and the adjusted wheel center trajectory. The wheel center height trajectory is vertically adjusted to compare with the original terrain profile. The terrain profile is smoothed due to the tire bridging and enveloping properties with respect to the undulations. For example, Figure 9 demonstrates that deep narrow cracks are filtered out of the resulting profile. In future work, a quantitated parameter identification process will be developed to determine the deformed shape parameters α_1 and α_2 quantitatively instead of trial and error. The tire constraint model will be further improved so that it can be applied on not only deterministic road profiles, but also to stochastic terrain profiles and ultimately to deformable terrain.

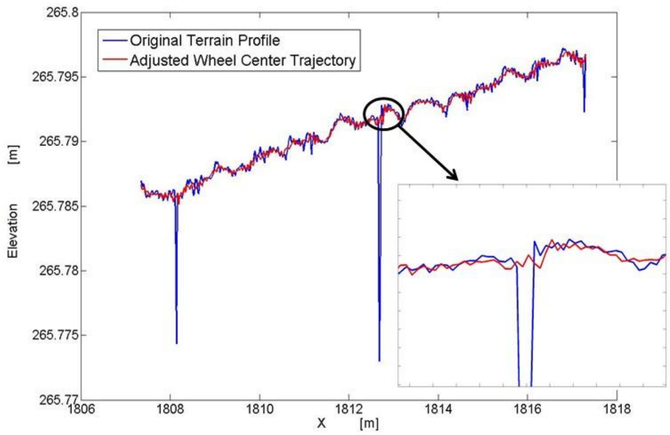

FIGURE 9. CONSTRAINT MODE FILTER.

CONCLUSIONS

The main contributions of this work are the enhancement to the constraint mode formulation for the tire-terrain interface and the development of the two tire shape parameters, α_1 and α_2, and an independent tire stiffness parameter, k_0. With this detailed expression of the model parameters, a model parameter identification process for tire constraint mode is established using only the flat plate results. A table with typical tire shape and stiffness parameters is provided. The model is shown to have bridging and enveloping properties over cracks and bumps, respectively. Reasonable predictions for the spindle force during a cleat test are demonstrated and the discontinuity in the stiffness during the cleat test is properly identified. This planar model can be used to predict the tire shape and the force acting on the spindle given a specific tire and a section of terrain profile. It can also serve as a morphological pre-filter of actual terrain to obtain the trajectory of the wheel center given constant load acting on the spindle.

ACKNOWLEDGEMENTS

The authors wish to thank Professor Schalk Els of the University of Pretoria for providing the experimental data used throughout this work. The Automotive Research Center (ARC), a U.S. Army center of excellence in modeling and simulation of ground vehicles, is gratefully acknowledged for their continued support of this research.

REFERENCES

[1] Umsrithong, A., *Stochastic Semi-Empirical Transient Tire Models*, in *Mechanic Engineering*. 2012, Virginia Tech: Blacksburg, VA.

[2] Badalamenti, J., M., Doyle jr., G., R., *Radial-interradial Spring Tire Models, Acoustic, Stress and Reliability in Design.* Journal of Vibration, 1988. **110**(1): p. 70-75,

[3] Zegelaar P., W., A., Pacejka, H., B., *The In-plane Dynamics of Tyres on Uneven Roads.* Vehicle System Dynamics, 1996: p. 714-730 10.1080/00423119608969231.

[4] Loo, M., *A Model Analysis of Tire Behavior under Vertical Loading and Straight-Line Free Rolling.* Tire Science and Technology, 1985. **13**(2): p. 67-90,

[5] Gillespie, T., D., *Fundamentals of Vehicle Dynamics*. 1992: Society of Automotive Engineers. 132 – 138.

[6] Takayama, M., Yamagishi, K., *Simulation Model of Tire Vibration.* Tire Science and Technology, 1984. **11**(1): p. 38 – 49, 10.2346/1.2150977.

[7] Ferris, J.B., *Capturing Planar Tire Enveloping Properties Using Static Constraint Modes*, in *ASME 2006 International Mechanical Engineering Congress and Exposition (IMECE2006), Dynamic Systems and Control Division* 2006: Chicago, Illinois, USA p. IMECE2006-15260 pp. 467-472

[8] Hurty, W.C., *Dynamic Analysis of Structural Systems Using Component Modes.* AIAA Jounrnal, 1965. **3**(4): p. 678-685,

[9] Gladwell, G.M.L., *Banch Mode Analysis of Vibrating Systems.* Journal of Sound and Vibration, 1964. **1**(1): p. 41-59,

[10] Guyan, R.J., *Reduction of Stiffness ans Mass Matrices.* AIAA Jounrnal, 1965. **3**(2): p. 380,

[11] Kuhar, E.J.S., C. V. , *A dynamic transformation method for modal synthesis.* . AIAA Jounrnal, 1973. **12**(5): p. 672-678,